Wear Characteristics of TiNi Shape Memory Alloys

H.C. LIN, H.M. LIAO, J.L. HE, K.C. CHEN, and K.M. LIN

The wear characteristics of TiNi shape memory alloys against Cr-steel have been studied. Experimental results indicate that the $Ti_{49}Ni_{51}$ alloy can exhibit a better wear resistance than $Ti_{50}Ni_{50}$ alloy due to their higher hardness and pseudoelastic behaviors. Four main mechanisms, adhesion, abrasion, surface fatigue, and brinelling, are found to have important contributions to the wear characteristics of TiNi alloys. The weight loss increases with increasing wear load and sliding distance but decreases with increasing sliding speed. The contact area during sliding wear will be increased due to the variant accommodation and/or pseudoelasticity and, hence, will reduce the average compressive stress and wear damage. Variant accommodation and/or pseudoelasticity can also stabilize the crack tips and hinder crack propagation, hence improving the wear characteristics of TiNi alloys.

I. INTRODUCTION

THE TiNi alloys are known as the most important shape memory alloys because of their many applications based on the shape memory effect[1] and pseudoelasticity.[2,3] This comes from the fact that TiNi alloys have superior properties in fatigue,[4] corrosion resistance,[5] biocompatibility,[6] ductility, and recoverable strain.[1] It is also well known that TiNi alloys can exhibit a high mechanical damping due to the easy movement of twin boundaries.[7,8] In addition to these functional properties, TiNi alloys have recently been observed to exhibit excellent wear resistance,[9–12] which is ascribed to their pseudoelastic behavior and hardening phenomenon. Suzuki and Kuroyanagi[13] and Shida and Sugimoto[14] also reported that the TiNi alloys exhibit good slurry and water jet erosion resistance in corrosive environment. Hence, TiNi alloys may become a new type of tribomaterial in some new applications. However, our understanding in this area is incomplete. No systematic investigation has been reported on the tribology of TiNi alloys. In the present study, we aim to investigate the wear characteristics of TiNi alloys under dry sliding, including wear mechanisms, morphologies of worn surfaces, and factors influencing the sliding wear. Meanwhile, deformation phenomena and phase transformations during sliding wear process are also discussed.

II. EXPERIMENTAL PROCEDURE

The conventional tungsten arc-melting technique was employed to prepare the $Ti_{50}Ni_{50}$ and $Ti_{49}Ni_{51}$ alloys. The as-melted buttons were homogenized at 1050 °C for 24 hours, hot rolled into plates with a 5-mm thickness, annealed at 800 °C for 30 minutes, and then quenched in water. The differential scanning calorimetry (DSC) measurement of transformation temperatures was conducted using a DU PONT* 2000 thermal analyzer equipped with a quantitative scanning system, 910 DSC cell, and a cooling accessory, LNCA II. Measurements were carried out at temperatures ranging from −150 °C to +150 °C under a controlled cooling/heating rate of 10 °C/min. A ball-on-disk type of apparatus with ASTM standard was used to test the specimen's wear resistance. The testing parameters include wear load, sliding distance, and sliding speed. The SUJ-2 Cr-steel ball, with hardness Hv = 720, was used as the against-wear material. The average friction coefficient was automatically calculated by a digit computer after the sliding wear process. The X-ray diffraction (XRD) analysis was carried out at room temperature with a MAC-MXP-3 X-ray diffractometer under the conditions of Cu K_α radiation, 40 kV tube voltage, and 30 mA current. The surface morphologies were observed by a Topcon ABT-55 scanning electron microscope with an energy-dispersive X-ray analysis facility. The surface hardness was measured with a microvickers tester with a load of 500 g for 15 seconds. For each specimen, the average hardness value was calculated from at least five test readings.

*DU PONT is a trademark of E.I. Du Pont de Nemours & Co., Inc., Wilmington, DE.

III. RESULTS AND DISCUSSION

A. *Metallurgical Properties Influencing the Wear Characteristics in TiNi Alloys*

To investigate the wear characteristics of TiNi alloys, it is helpful to first understand some important metallurgical properties of these alloys. Table I presents the transformation temperatures, hardness, and crystal structures at room temperature for both $Ti_{50}Ni_{50}$ and $Ti_{49}Ni_{51}$ alloys. Based on tribological theory,[15] materials with high hardness exhibit high wear resistance. However, it is quite interesting to find that the hardness of TiNi alloys, as presented in Table I, is so much lower compared to commercial wear-resistant materials,[9] but the alloys can exhibit excellent wear resistance. Hence, not only the hardness, but also the other metallurgical properties, such as phase transformations, work hardening, and resistance to crack nucleation and propagation, will have important influence on the wear characteristics of TiNi alloys. It is well known that the TiNi

H.C. LIN, J.L. HE, and K.C. CHEN, Associate Professors, H.M. LIAO, Graduate Student, and K.M. LIN, Professor, are with the Department of Materials Science, Feng Chia University, Taichung, Taiwan 407, Republic of China.

Manuscript submitted November 18, 1996.

Table I. The Transformation Temperatures, Hardness, and Crystal Structure at Room Temperature for Both $Ti_{50}Ni_{50}$ and $Ti_{49}Ni_{51}$ Alloys

Alloy	M* (°C)	A* (°C)	Hardness (Hv)	Crystal Structure
$Ti_{50}Ni_{50}$	46	82	200	B19' martensite
$Ti_{49}Ni_{51}$	−104	−60	320	B2 parent phase

martensite can be preferentially reoriented to accommodate the deformation strain. This phenomenon will release the stress concentration around the crack tips and, hence, hinder crack propagation. Meanwhile, the pseudoelastic behavior originating from the stress-induced martensitic transformation of the parent B2 phase will increase the elastic contact area and reduce the normal stress during sliding. All these unique properties of TiNi alloys are considered to be responsible for the alloys' high wear resistance. Hence, the transformation temperatures and the pre-existing structures will considerably influence the wear characteristics of TiNi alloys.

B. *Morphologies of Worn Surfaces in TiNi Alloys*

Four main wear mechanisms, adhesion, abrasion, surface fatigue, and brinelling, are observed during sliding wear tests of TiNi alloys against Cr-steel. Some morphologies of these worn surfaces are shown in Figures 1(a) through (d). As can be seen in Table I, the TiNi alloys are so much softer than Cr-steel (Hv = 720); hence, adhesive wear will produce fragments of TiNi alloys (Figure 1(a)), which adhere to the surface of Cr-steel. Figures 2(a) and (b) show the scanning electron microscopy (SEM) observation and energy-dispersive X-ray analysis of the adhesive protrution on the surface of Cr-steel, respectively. As shown in Figure 2(b), there are intense Ti and Ni peaks appearing together with Fe peak. These features provide direct evidence that TiNi fragments transfer to the Cr-steel surface because of adhesion during sliding wear. The ploughing grooves in Figure 1(b) illustrate abrasive wear, which originates from the interaction of microcutting and plastic deformation.[16] Surface fatigue wear is also observed in Figure 1(c). Due to the repeated loading and unloading cycles, many surface or subsurface cracks form and eventually result in the breakup of the surface into large fragments, leaving large pits on the surface, as shown in Figure 3. At the same time, Figure 1(d) shows the wavy tracks in the outer surface. This feature, so-called brinelling wear, occurs from the plastic deformation of softer materials. It should be mentioned that the phenomenon of brinelling wear will increase the friction coefficient, but it has little contribution to the weight loss. Meanwhile, the brinelling wear in $Ti_{49}Ni_{51}$ alloy, being ascribed to its higher hardness, is slighter than that of $Ti_{50}Ni_{50}$ alloy.

C. *Factors Influencing the Wear Characteristics of TiNi Alloys*

As well as the metallurgical properties, many testing parameters, *e.g.*, the wear load, sliding distance, and sliding speed in this study, can influence the wear characteristics of TiNi alloys.

Fig. 1—Morphologies of worn surfaces of TiNi alloys: (*a*) adhesive, (*b*) abrasive, (*c*) surface fatigue, and (*d*) brinelling.

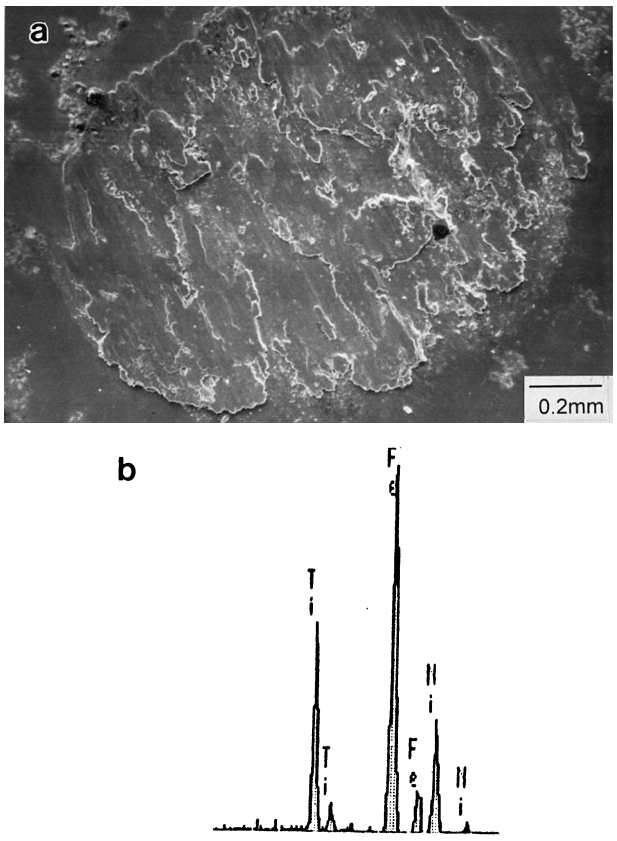

Fig. 2—(*a*) SEM observation and (*b*) EDX analysis of the adhesive protrution on the surface of Cr steel.

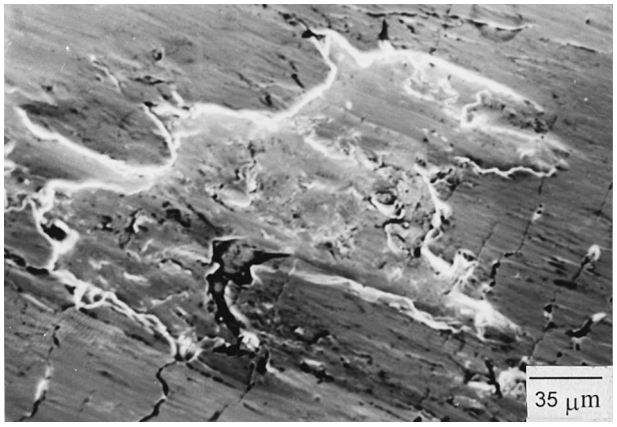

Fig. 3—SEM observation showing the large pit on the worn surface.

1. *Wear load*

Figures 4(a) and (b) show the experimental results of weight loss and friction coefficient, respectively, as a function of wear load for both $Ti_{50}Ni_{50}$ and $Ti_{49}Ni_{51}$ alloys. As expected from its higher hardness, the $Ti_{49}Ni_{51}$ alloy can exhibit a better wear resistance than that of the $Ti_{50}Ni_{50}$ alloy, namely, lower weight loss and friction coefficient, as shown in Figures 4(a) and (b), respectively. Meanwhile, the weight loss increases with the increasing wear load. These experimental results obey Archard's law:[17]

$$R = K\,(P/H)\,v$$

where R, K, P, H, and v denote, respectively, wear rate

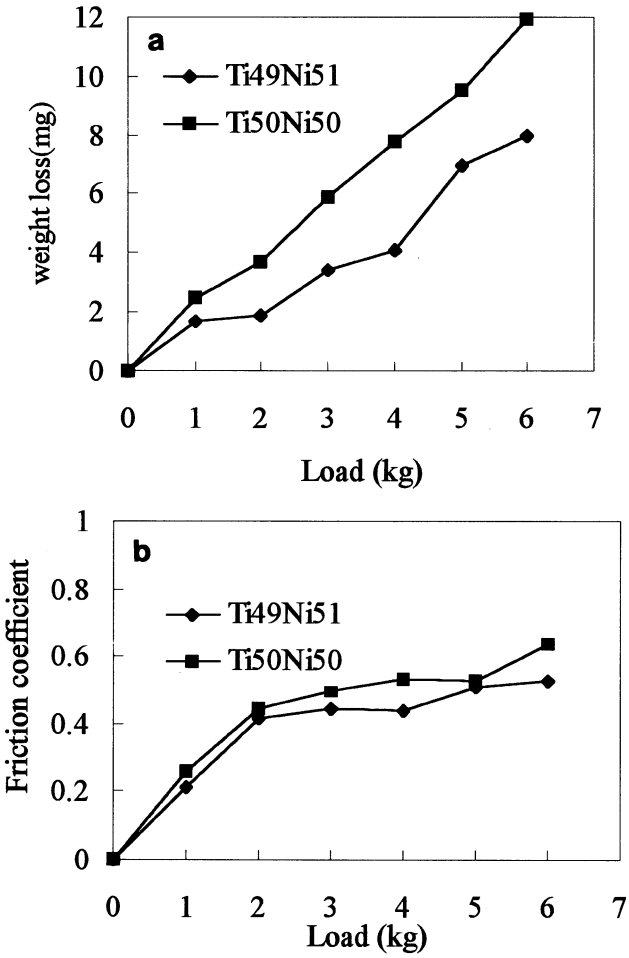

Fig. 4—(*a*) Weight loss and (*b*) friction coefficient, as a function of wear load for both $Ti_{50}Ni_{50}$ and $Ti_{49}Ni_{51}$ alloys.

(volume/time), wear coefficient, pressure, hardness, and velocity. Namely, the wear rate is proportional to P (or wear load in this study), but inversely proportional to hardness, as shown in Figure 4(a). Figures 5(a) through (d) show the worn surface morphologies and their illustrated diagrams at 2- and 6-kg wear loads for the $Ti_{50}Ni_{50}$ alloy. The appearance of a large quantity of fatigue cracks and surface pits in Figures 5(a) and (b) indicates that the surface fatigue is quite an important wear mechanism for TiNi alloys. In fact, these fatigue cracks exhibit different morphologies at various wear loads. As shown in Figures 6(a) and (b), the fatigue cracks at low wear loads are short and dense due to the lower repeated stress, but the cracks at high wear loads are long and deep due to the rapid extension under higher repeated stress. The pearl-like crests appearing in Figures 5(c) and (d) should be ascribed to the accumulation of adhesive junction, abrasive deformation, and wear chips and the mechanical locking of surface pits. These pearl-like crests will increase the fluctuation of friction coefficient during sliding wear process and rapidly increase the wear rate due to mechanical fracture. The worn surface morphologies at various wear loads for $Ti_{49}Ni_{51}$ alloy are similar to those for $Ti_{50}Ni_{50}$ alloy, but there are fewer fatigue cracks and surface pits for $Ti_{49}Ni_{51}$ alloy and the pearl-like crests are not so obvious as for $Ti_{50}Ni_{50}$ alloy. These features may stem from the fact that $Ti_{49}Ni_{51}$ alloy has higher hardness.

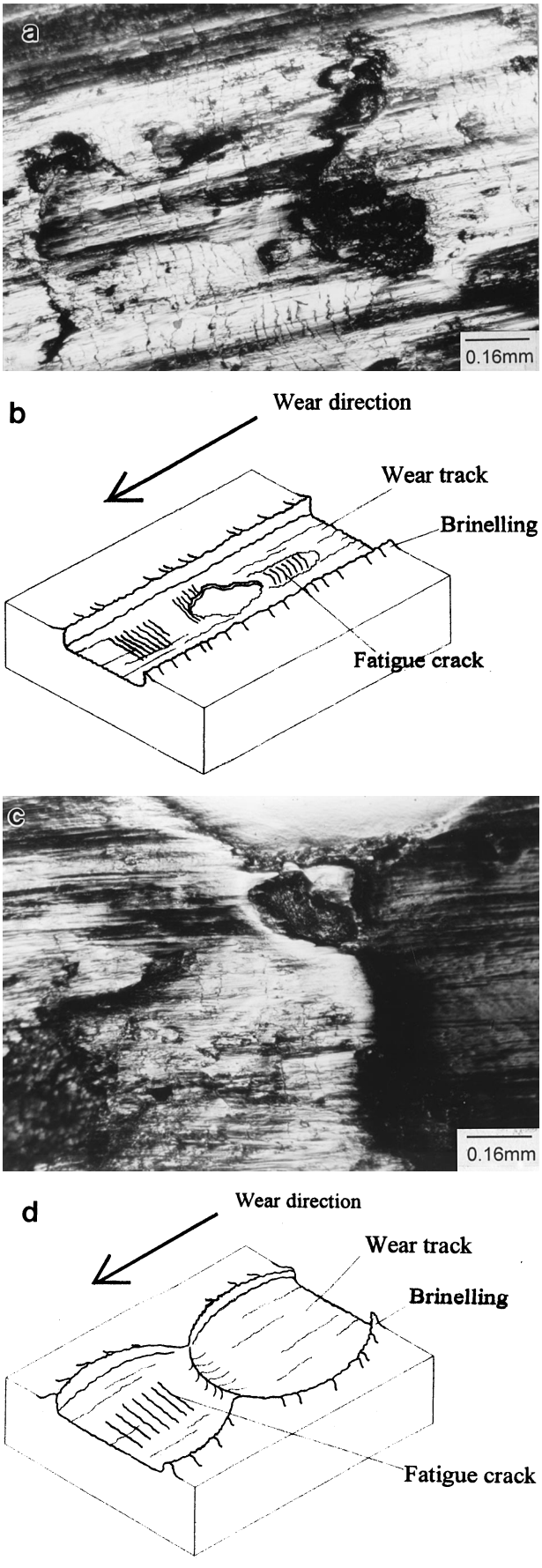

Fig. 5—Worn surface morphologies and illustrated diagrams for $Ti_{50}Ni_{50}$ alloy: (*a*) 2-kg wear load, (*b*) illustrated diagram of (a), (*c*) 6-kg wear load, and (*d*) illustrated diagram of (c).

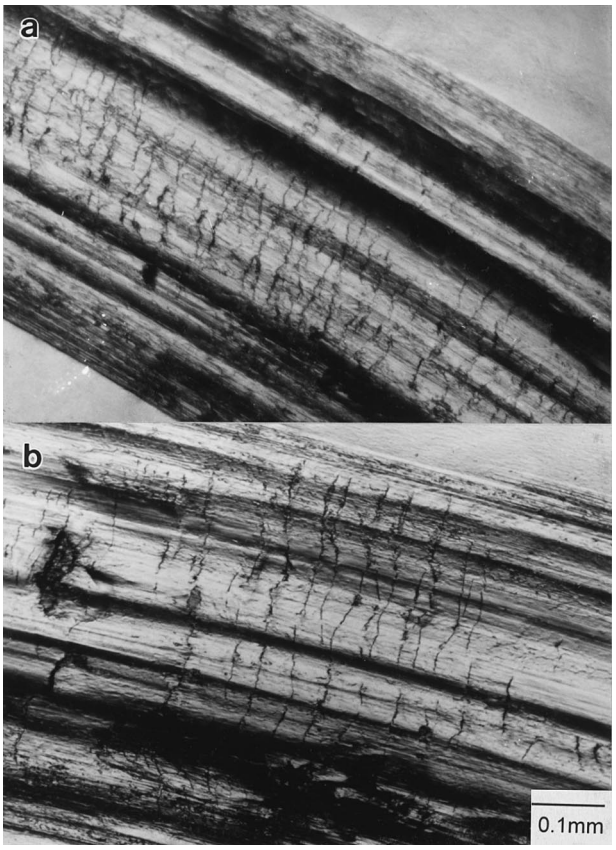

Fig. 6—Surface cracks at (*a*) low wear load and (*b*) high wear load.

2. *Sliding distance*

Figures 7(a) and (b) show the experimental results of weight loss as a function of sliding distance at various wear loads for $Ti_{50}Ni_{50}$ and $Ti_{49}Ni_{51}$ alloys, respectively. From Figures 7(a) and (b), the weight losses are found to increase with increasing sliding distance, especially for higher sliding distance. The interaction among wear mechanisms is expected to accelerate the wear rate. As shown in Figures 8(a) and (b) for the $Ti_{50}Ni_{50}$ alloy subjected to 500-m sliding at 4-kg wear load, the fatigue cracks, which rapidly grow into the subsurface, will link together to break up some fragments and then leave some pits on the surface. These pits will increase the friction coefficient and induce the mechanical fracture. Besides, the wear chips retained in the worn tracks will also increase the abrasive wear. All these features will accelerate the wear rate.

3. *Sliding speed*

Figure 9 shows weight loss as a function of sliding speed for both $Ti_{50}Ni_{50}$ and $Ti_{49}Ni_{51}$ alloys. In Figure 9, one can find that the weight loss decreases with increasing sliding speed for both $Ti_{50}Ni_{50}$ and $Ti_{49}Ni_{51}$ alloys. Strain rate hardening[18] is considered to be responsible for this phenomenon. As shown in Figure 10, the specimen's effective hardness increases with increasing sliding speed. This indicates that at constant wear load, high strain rate will reduce the deformation strain because of the hardening effect and, hence, reduce the wear rate. Meanwhile, it is worthy to mention that the worn surface has dense and short fatigue cracks at high sliding speeds, but has deep and long fatigue cracks at low sliding speeds. These deep and long fatigue

cracks will also increase the wear rate, and hence, there is a higher weight loss at lower sliding speed.

D. *Deformation Phenomena during Sliding Wear of TiNi Alloys*

In order to reveal more clearly the deformed structures induced by sliding wear, XRD results are shown in Figures 11 and 12 for $Ti_{50}Ni_{50}$ and $Ti_{49}Ni_{51}$ alloys, respectively. Typical XRD spectra for as-annealed TiNi martensite are shown in Figure 11(a). After sliding wear tests, as shown in Figure 11(b) through (d), the line intensity of martensite spectra decreases, but the parent B2 phase gradually appears with increasing wear load. Eventually, only a broad XRD peak of parent B2 phase appears if the wear load exceeds 5 kg. As reported in a previous article,[19] the stress-induced parent phase (SIP) can be introduced by cold rolling due to the complex stress distribution. In the present study, as shown in Figure 11, the SIP can also be introduced during the sliding wear. These SIP will enhance the wear resistance of TiNi martensite by their pseudoelastic behavior. In Figure 12, the XRD peak of the parent B2 phase is broadened due to the residual strain after the sliding wear test. An ambiguous XRD peak of stress-induced martensite (SIM) is observed in Figure 12(d) for the 5-kg-load specimen, although most of the SIM is recovered to the parent B2 phase.

E. *The Compressive Stress and Surface Temperature in the Contact Area*

Table II presents the calculated Hertzian compressive stress[20] in the contact area at various wear loads and yield stresses for both the martensite and parent B2 phase of TiNi alloys. As presented in Table II, all the calculated Hertzian compressive stresses at 1- to 7-kg wear loads exceed the yield stresses of TiNi martensite and parent B2 phase. This indicates that plastic deformation in both martensite and parent B2 phase will occur during all the sliding wear processes. This plastic deformation will significantly affect the wear characteristics of TiNi alloys, as discussed in Section D.

It is also important to know the surface temperature around the contact area during the sliding wear process. The temperature in the contact area can be theoretically calculated by using the Cowan equation.[21] Based on this theoretical calculation, the instantaneous surface temperatures at various wear loads (1 to 6 kg) and sliding speeds (100 to 600 rpm) are in the range of 80 °C to 450 °C. All these calculated instantaneous surface temperatures exceed the reverse martensitic transformation temperatures (A_s) for $Ti_{50}Ni_{50}$ martensite. This indicates that some martensite on the contact area has been reversely transformed to parent B2 phase. However, Figure 13 shows the measured surface temperatures near the contact area, just about 1 mm from the contact area. These measured temperatures are all well below 50 °C. This feature means that there is a rapid reduction of surface temperatures. Hence, it is reasonable to suppose that the heat-affected zone during the sliding wear in this study is limited. Namely, most of the wear tracks and subsurfaces still exhibit the martensite structure. Meanwhile, the reversely transformed parent B2 phase will forwardly transform to martensite again due to the rapid cooling to below the M_s temperature. This martensite will wear against Cr-steel ball during the next cycle.

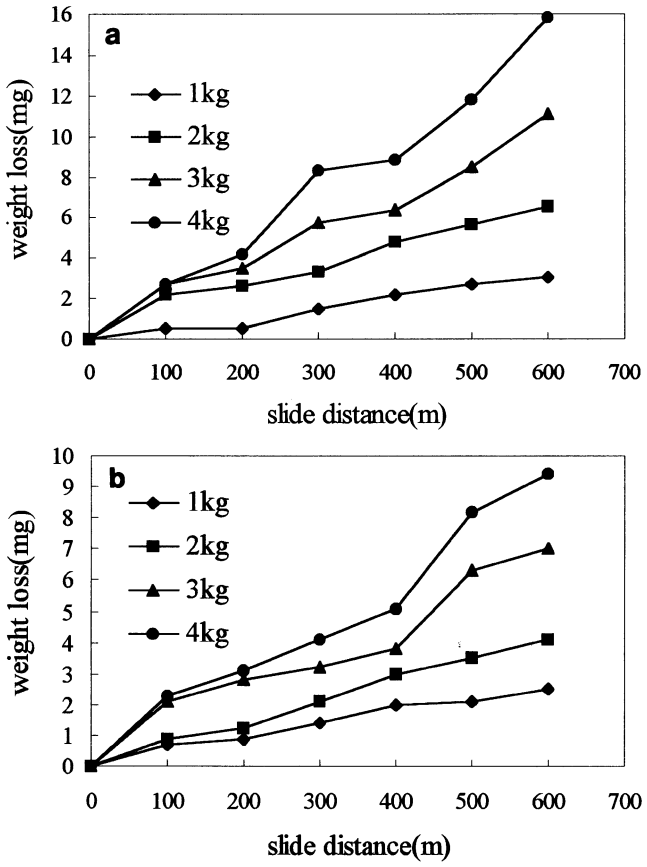

Fig. 7—The weight loss as a function of sliding distance for (*a*) $Ti_{50}Ni_{50}$ and (*b*) $Ti_{49}Ni_{51}$ alloys.

F. *The Effects of Thermoelastic Martensitic Transformations on the Wear Characteristics of TiNi Alloys*

It is interesting to find that the wear characteristics of TiNi alloys are so favorable, namely, they have high wear resistance although their hardness is soft. These unusual wear characteristics are believed to be related to their thermoelastic behaviors. During the sliding wear of TiNi martensite, partial strain energy has been annihilated by variant accommodation. The accommodated martensite will absorb the friction heat during the sliding wear and then reversely transform to parent B2 phase. This feature will improve the wear characteristics of TiNi martensite due to the reduction of surface temperature and introduction of wear-resistant B2 phase. In the parent B2 phase of TiNi alloys, the applied strain during sliding wear process will be mostly transformed to elastic strain due to the formation of SIM. This elastic strain will not induce the wear damage. The SIM will recover to their parent B2 phase after the relief of applied load. The thermoelastic martensitic transformations of TiNi alloys make two other important contributions because of their wear characteristics. First, the contact area during sliding wear will be increased due to the variant accommodation and/or pseudoelasticity. This phenomenon will reduce the average compressive stress and, hence, reduce the wear damage. Second, the fatigue crack tips can be

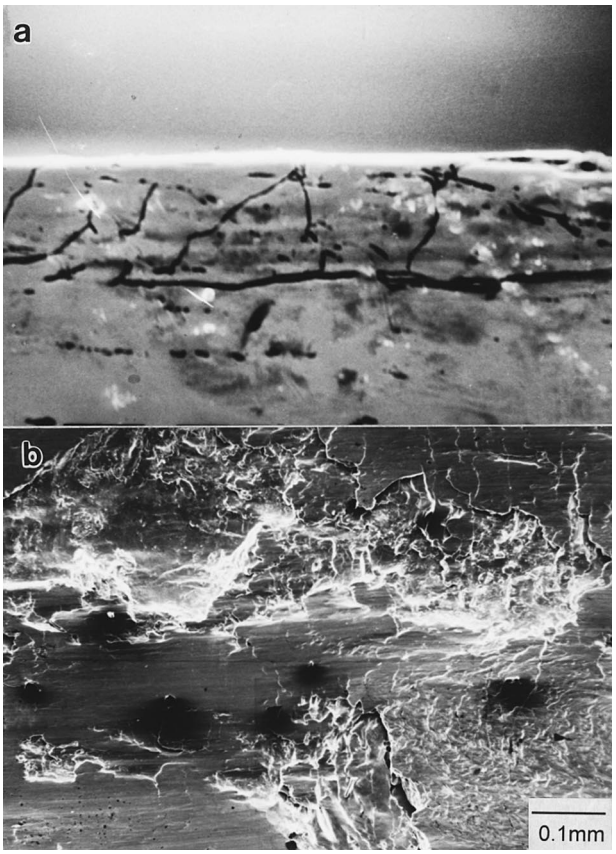

Fig. 8—(*a*) Cross-sectional observation showing the linkage of fatigue cracks in the subsurface. (*b*) Top surface showing many surface pits.

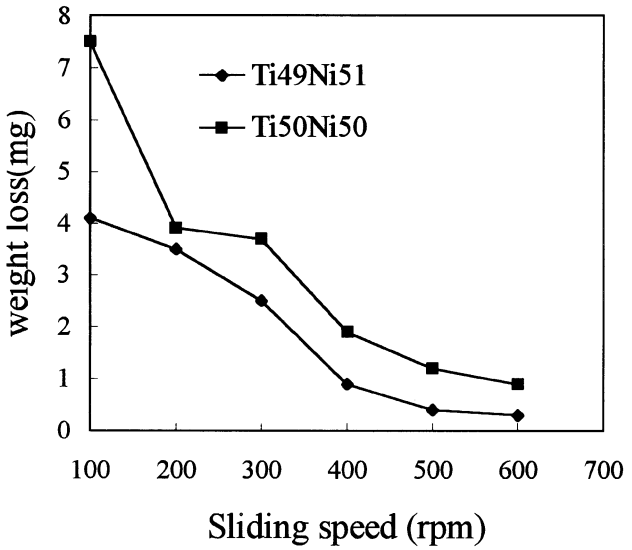

Fig. 9—Weight loss as a function of sliding speed for both $Ti_{50}Ni_{50}$ and $Ti_{49}Ni_{51}$ alloys.

stabilized due to stress relief by the variant accommodation and/or pseudoelasticity. For common metals and alloys, the strain energy of crack tips is always released by plastic deformation and/or crack propogation. However, for TiNi alloys, the variant accommodation and/or pseudoelasticity will absorb partial strain energy to store in the martensite variants and/or SIM. These unstable martensite variants and SIM will recover to parent B2 phase, because the instantaneous surface temperature is higher than the A_s temperature during sliding wear process. These phenomena will stabilize the crack tips and hinder the crack propogation, hence improving the wear characteristics of TiNi alloys.

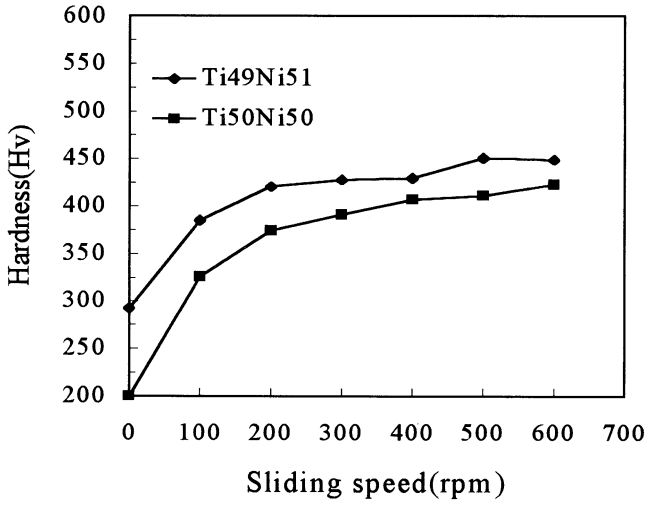

Fig. 10—Hardness as a function of sliding speed for both $Ti_{50}Ni_{50}$ and $Ti_{49}Ni_{51}$ alloys.

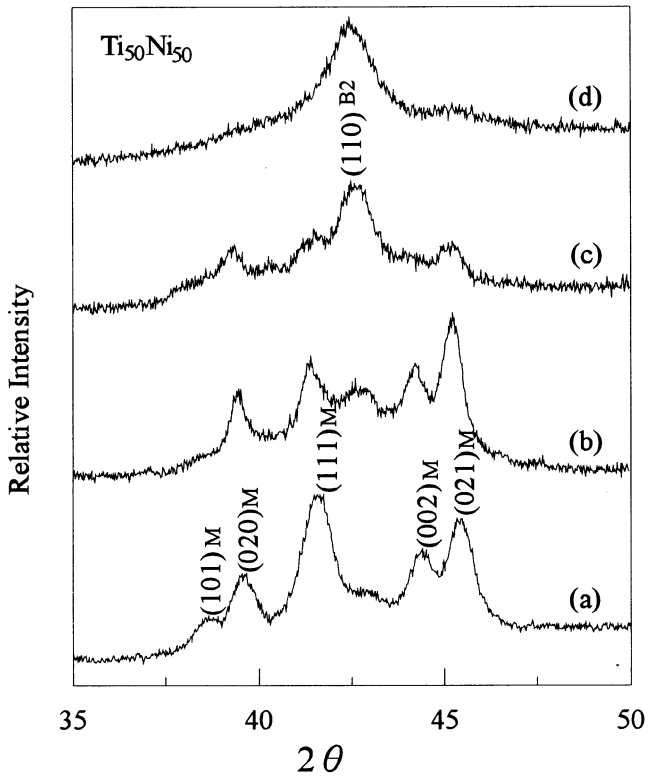

Fig. 11—XRD spectra for (*a*) as anneal and for the worn $Ti_{50}Ni_{50}$ alloy under (*b*) 1-kg load, (*c*) 3-kg load, and (*d*) 5-kg load.

IV. CONCLUSIONS

1. The $Ti_{49}Ni_{51}$ alloy exhibits better wear resistance than the $Ti_{50}Ni_{50}$ alloy due to higher hardness and pseudoelastic behaviors.
2. Four main mechanisms, adhesion, abrasion, surface fa-

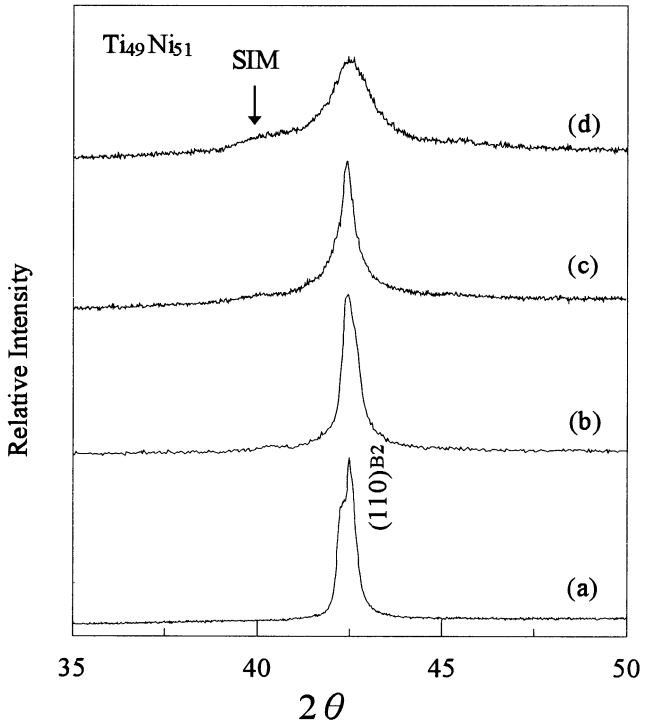

Fig. 12—XRD spectra for (*a*) as anneal and for the worn $Ti_{49}Ni_{51}$ alloy under (*b*) 1-kg load, (*c*) 3-kg load, and (*d*) 5-kg load.

Table II. The Calculated Hertzian Compressive Stress in the Contact Area at Various Wear Loads for Both Martensite and Parent B2 Phase

Wear Load (kg)	Hertzian Compressive Stress (10^8 N/m^2)	
	Martensite	B2
1	2.22 to 2.86	4.58
2	2.80 to 3.61	5.77
3	3.20 to 4.13	6.61
4	3.53 to 4.55	7.28
5	3.80 to 4.90	7.84
6	4.04 to 5.20	8.30
Yield stress	0.7×10^8 N/m^2	2×10^8 N/m^2

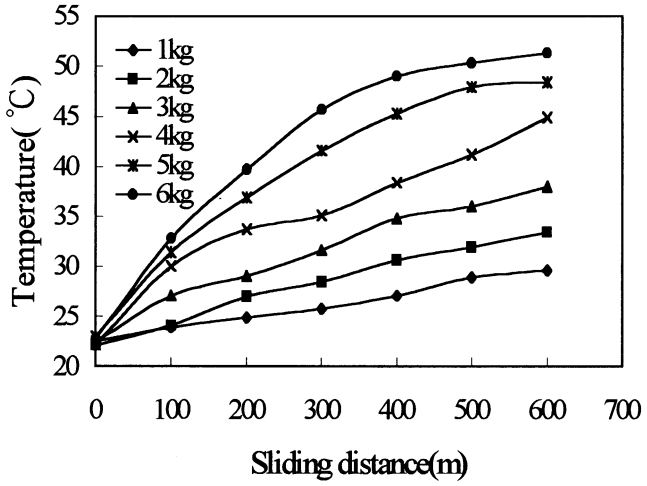

Fig. 13—The measured surface temperature as a function of sliding distance at various wear loads for $Ti_{50}Ni_{50}$ alloy.

tigue, and brinelling, are found to have important contributions to the wear characteristics of TiNi alloys.

3. As well as the metallurgical properties, wear load, sliding distance, and sliding speed all have considerable influence on the wear characteristics of TiNi alloys. The weight loss increases with increasing wear load and sliding distance, but decreases with increasing sliding speed.
4. The SIP can be introduced during the sliding wear process and enhance the wear resistance of TiNi alloys.
5. The thermoelastic martensitic transformations of TiNi alloys have important effects on their wear characteristics. The contact area during sliding wear will be increased due to the variant accommodation and/or pseudoelasticity and, hence, reduce the average compressive stress and wear damage. The variant accommodation and/or pseudoelasticity can also stabilize the crack tips and hinder the crack propogation, hence improving the wear characteristics of TiNi alloys.

ACKNOWLEDGMENTS

The authors are pleased to acknowledge the financial support of this research by the National Science Council (NSC), Republic of China, under NSC Grant No. 86-2216-E-035-015. The authors also express their sincere appreciation to Professor S.K. Wu, Institute of Materials Science and Engineering, National Taiwan University (Taipei, Taiwan), for his kind assistance with the use of experimental equipment.

REFERENCES

1. S. Miyazaki, K. Otsuka, and Y. Suzuki: *Scripta Metall.*, 1981, vol. 15, pp. 287-92.
2. S. Miyazaki, Y. Ohmi, K. Otsuka, and Y. Suzuki: *Proc. ICOMAT-82, J. Phys.*, 1982, vol. 43, pp. C4-255-C4-260.
3. S. Miyazaki, T. Imai, Y. Igo, and K. Otsuka: *Metall. Trans. A*, 1986, vol. 17A, pp. 115-20.
4. K.N. Melton and O. Mercier: *Acta Metall.*, 1979, vol. 27, pp. 137-44.
5. Y. Oshida and S. Miyazaki: *Corr. Eng.*, 1991, vol. 40, pp. 1009-25.
6. L.S. Castleman and S.M. Motzkin: in *Biocompatibility of Clinical Implant Materials*, D.F. Williams, ed., CRC Press, Boca Raton, FL, 1981, pp. 129-54.
7. H.C. Lin, S.K. Wu, and M.T. Yeh: *Metall. Trans. A*, 1993, vol. 24A, pp. 2189-94.
8. H.C. Lin, S.K. Wu, and Y.C. Chang: *Metall. Mater. Trans. A*, 1995, vol. 26A, pp. 851-58.
9. J.L. Jin and H.L. Wang: *Acta Metall. Sinica*, 1988, vol. 24, pp. A66-A69.
10. D.Y. Li: *Scripta Metall.*, 1996, vol. 34, pp. 195-200.
11. P. Clayton: *Wear*, 1993, vols. 162-164, pp. 202-10.
12. J. Singh and A.T. Alpas: *Wear*, 1995, vols. 181–183, pp. 302-11.
13. Y. Suzuki and T. Kuroyanagi: *FAEDIC-NT, Titanium Zirconium*, 1979, vol. 27, pp. 67-73.
14. Y. Shida and Y. Sugimoto: *Wear*, 1991, vol. 146, pp. 219-28.
15. J. Halling: *Introduction to Tribology*, Wykehan Publications Ltd., London, 1976.
16. O. Vingsbo: *Wear of Materials*, ASME, New York, NY, 1979, pp. 620-35.
17. I.M. Hutchings: *Tribology: Friction and Wear of Engineering Materials*, CRC Press, Boca Raton, FL, 1992, pp. 82-85.
18. T.H. Courtney: *Mechanical Behavior of Materials*, McGraw-Hill Publishing Co., New York, NY, 1990, pp. 16-17.
19. H.C. Lin and S.K. Wu: *Metall. Trans. A*, 1993, vol. 24A, pp. 293-99.
20. R.S. Cowan and W.O. Winer: in *ASM Handbook*, vol. 18, *Friction, Lubrication, and Wear Technology*, P. Blau, ed., Materials Park, OH, 1992, p. 39.
21. I. Kleis: *Z. Werkstofftech.*, 1984, vol. 15, pp. 49-58.